

# **A FRAMEWORK FOR AUTOMATED ROCK SEGMENTATION OF THE MARS EXPLORATION ROVER IMAGERY**

**Yong-hak Song**                      **Jie Shan**

Geomatics Engineering, School of Civil Engineering

Purdue University, 550 Stadium Mall Drive

West Lafayette, IN 47907, USA, Phone: +1-765-494-2168, Fax: +1-765-496-1105

{song10, jshan}@ecn.purdue.edu

## **ABSTRACT**

Rock segmentation (detection) is an important function required for the success of the Mars Exploration Rover mission and its scientific studies. In this paper, a general framework for automated rock detection using texture based multi-resolution image segmentation is developed and implemented. Three schemes, wavelet based local transform, multi-resolution histograms, and inter-scale decision fusion are combined and applied. Two test images taken by the panorama camera on rover Spirit at the Gusev Crater landing site are used to evaluate the performance of the proposed framework. This paper presents the theory, implementation details and the test results of two MER Spirit images.

## **INTRODUCTION**

One of the objectives of the Mars Exploration Rover (MER) mission is to map the rocks and soils at the landing sites that might hold clues to past water activity. It is therefore necessary to develop an automated approach to extract the rocks from the images taken by the rovers. Such capability is useful for effective rover navigation, rock measurement and characterization, landing site mapping and ground truth collection for future exploration missions.

There have been a number of efforts towards rock detection. In 1994, Crida and Jager propose a knowledge based approach for rock recognition based on K-nearest neighbor classification. It is a good first step for rock detection but needs a lot of pre-information to determine the clustering threshold. Recently, many works are reported in autonomous rock detection due to the mars exploration rover mission. Gor et al (2001) integrate intensity data and range data by using unsupervised classification. This algorithm requires image scale as a significant control parameter. Castano et al (2004) detect rocks using boundary edges. Different strategies are used according to the size of rocks. For small rocks, Sobel and Canny edge detectors are applied, and the rocks are found by searching small closed shapes. For large rocks, the image is first downsampled before the above procedure is implemented. When rocks are detected at both high and low resolutions, the ones detected at the highest resolution are retained. On the other hand, if rocks are detected only at the low resolution, they refit the boundary using active contour. In 2005, Thompson uses multi-band segmentation approach with color image. They create three image bands from the color image using hue, saturation and intensity. Rocks are detected by using both supervised and unsupervised classification. However, the difficulty remains that a rock may have non-homogeneous intensity and color, which vary in terms of illumination and geometry of rock surface.

The study presented in this paper detects rocks using texture-based image segmentation and multi resolution clustering. The approach consists of three schemes: wavelet based local transform, texture evaluation utilizing the multi-resolution histograms, and inter-scale decision fusion for unsupervised classification based on the interactive K-means clustering.

## **SEGMENTATION PRINCIPLES**

Image segmentation is to assign a class label to each pixel of an image according to the properties of the pixel. Because of their complex geometries, rocks can not be segmented by only using intensity information and therefore texture is to be exploited. Texture is defined as an attribute representing the spatial arrangement of gray levels in a region (IEEE, 1990). In case of using the spatial location and relationship between pixels instead of the pixels themselves, it is considered as texture based image segmentation.

Textures can be modeled in different ways. Early approaches are focused on the analysis of the first or second order statistics, Gauss-Markov random field, local linear transforms and PCA (Principle Component Analysis). Kashyap et al (1996) develop a texture classification scheme based on autoregressive model. Although it can extract the rotation-invariant texture, it is not able to handle strong anisotropy texture. Cohen (1991) uses Gaussian-Markov random field and maximum likelihood method to model textures. The problem of this method is that the likelihood function is highly nonlinear and the algorithm needs high computational cost. Jain and Farrokhnia (1991) develop an unsupervised texture segmentation algorithm based on Gabor filters. It is now widely used along with wavelet transform. However, the proper filter design is required. Hadjidemetriou et al (2004) used multi-resolution histograms for texture analysis to overcome the limitation that single intensity histogram does not encode spatial information. The Gaussian filter is used to generate lower resolution images and the change of their intensity histograms is analyzed with respect to the resolution.

Even texture modeling is completed successfully, the size of the classification window remains to be another crucial problem in image segmentation. A large window usually enhances the classification reliability but may yield wrong classification. On the other hand, small window reduces the chance having wrong classified pixels but produces poor reliability due to scanty statistical information. For that reason, many segmentation algorithms employ the multi-resolution strategy (Fosgate et al, 1997; Li et al, 2000).

Once multiple resolutions are involved, a strategy must be developed to synergize or associate the results obtained across the different resolutions. Focusing on unsupervised classification, Salari and Ling (1995) tried texture segmentation using hierarchical wavelet decomposition. They applied the concept of inter-scale decision fusion to clustering technique. In this study, the segmentation result is refined in a coarse to fine fashion. The clustering results, called label value, in coarse image are added as elements of clustering input vector for finer image after normalization based on their mean and standard deviation value. In 2003, Vlachos et al introduced multi-resolution K-means clustering of time series for an online image search engine. They suggest interactive K-means algorithm to solve the two critical problems of K-means clustering: the significant computation complexity increase according to the dimensionality of data or the length of sequence, and the strong dependency of clustering quality in initial seed centers. They use the result of clustering in a lower resolution as the initial seed centers for clustering in a higher resolution and iterate this procedure until none of the objects changes membership. Also, this algorithm can allow users to interrupt the clustering at any level. Through this, users can control the balance between cost time and quality.

Based on the above discussions, we propose a multi-resolution texture-based rock segmentation framework. We first apply a wavelet transform as a local transform to decompose the input images into a sequence of low resolution (frequency) images and edge (high frequency) images. Histograms are then calculated for each wavelet transformed image window by window of a predefined size to retain the local properties of the images. In the next step, histogram changes of the corresponding images at different resolutions are examined and used as the texture measures. As a result, each window will obtain a texture vector that characterizes its texture properties determined from lower frequency and high frequency components across multiple resolutions. In the final step, such texture vectors of all windows will be used as input to an interactive K-means clustering to separate rocks from their background.

### **Local transform**

Local transform helps the extraction of various texture properties. Generally, the high frequency component of an image such as spot or edge can explain texture better than the low frequency component. As a matter of fact, intensity value is primary information for image segmentation but more accurate segmentation result can be expected if additional information from the local transform of image such as edge or spot detection operator is included. The wavelet decomposition converts the image into one downsampled low frequency image and three downsampled high frequency images in vertical, horizontal and diagonal directions. Hence we can use the high frequency images as additional information for segmentation.

### **Multi-resolution histograms**

The multi-resolution histograms are formed by generating a histogram for each of the lower resolution images obtained through wavelet transform. The change of histograms is then examined with respect to the image resolution. Such histogram change reflects the variation of spatial information and is measured by the generalized Fisher information content. As an example, Figure 1 shows histogram change with respect to resolutions. The two input images have the same mean and standard deviation at original resolution. However, as the images are changed from fine to coarse by the wavelet decomposition, each histogram has different pattern according to spatial distribution of pixels.

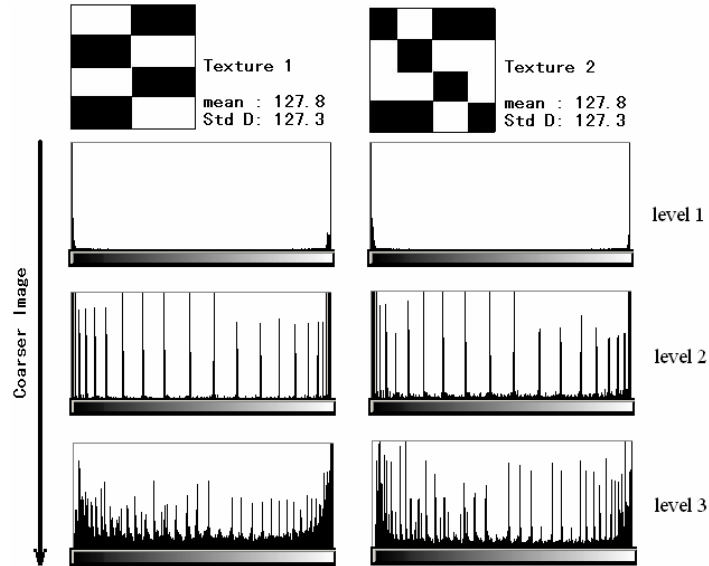


**Figure 1.** Multi resolution histograms

Using the multi resolution histograms we can evaluate textures through detecting the change of histogram according to the levels of the wavelet decomposition using the mean of histogram differences weighted by entropy of intensity of each bin as below

$$K_J = \sum_{i=0}^{m-1} -v_i \ln v_i \frac{h_i(L_J) - 4h_i(L_{J+1})}{\sum_{i=0}^{m-1} h_i(L_J)} \quad (1)$$

where

$L_J$  : wavelet approximate coefficient at level  $J$ , with 0 being the highest resolution;

$v_i$  : intensity of bin  $i$ ;

$m$ : number of bins;

$h_i$  : histogram bin count.

This  $K_J$  measures the histogram change between  $i$ -th level image  $L_J$  and  $(i-1)$ -th level image  $L_{J-1}$ . In this study, three histogram differences between four levels of images are used as a set of clustering input vectors. Such computation applies to each wavelet transformed component image.

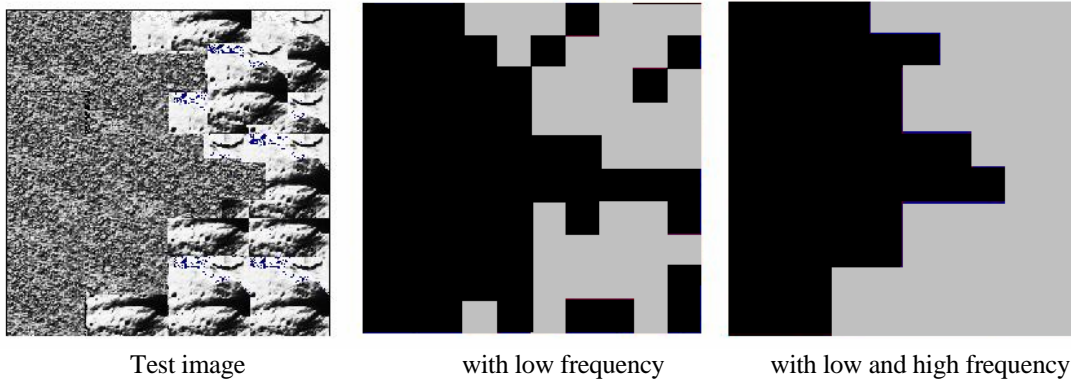


**Figure 2.** Segmentation results with inclusion of high frequency components

Shown in Figure 2 are the segmentation results from an 400 by 400 artificial image. The artificial image is first decomposed by wavelet transform to obtain a sequence of low and high frequency component images. Histogram changes are evaluated by using Equation 1 for each component image across the multiple resolutions. To retain the spatial properties of the textures, such evaluation is carried out based on a 40 by 40 window. The texture vectors obtained for each window are then used as input to the K-means clustering. The tests are performed to examine the improvement of using not only the low frequency but also other three high frequency images. As is shown, the inclusion of high frequency components improves the segmentation operation by providing more continuous and connected results.

### Clustering with inter-scale decision fusion

In this study, K-means clustering is applied as an unsupervised classification algorithm. This algorithm aims at minimizing an objective function (proximity function) as below

$$\Phi = \sum_{j=1}^k \sum_{i=1}^n \|x_i^{(j)} - c_j\| \quad (2)$$

$\|x_k^{(j)} - c_j\|$  is a chosen distance between a data point  $x$  and the cluster centre  $c$

$k$  : number of clusters

$n$  : number of data

The clustering with inter-scale decision fusion has two strategies: refining the clustering result of coarse image with fine image, and determining appropriate cluster for fine image from the coarse image. The K-means method is modified accordingly. Each set of input vector  $V$  at resolution level  $i$  for the clustering with inter-scale decision fusion is as below. The set of histograms at three different resolution levels are utilized in our study.

$$V_{i+0} = \begin{bmatrix} K'(L_{i+1}, L_{i+2}) \\ K'(L_{i+2}, L_{i+3}) \\ K'(L_{i+3}, L_{i+4}) \end{bmatrix}$$

$$\vdots \quad \quad \quad \vdots$$

$$V_{i+n} = \begin{bmatrix} K'(L_{i+n+1}, L_{i+n+2}) \\ K'(L_{i+n+2}, L_{i+n+3}) \\ K'(L_{i+n+3}, L_{i+n+4}) \end{bmatrix} \quad (3)$$

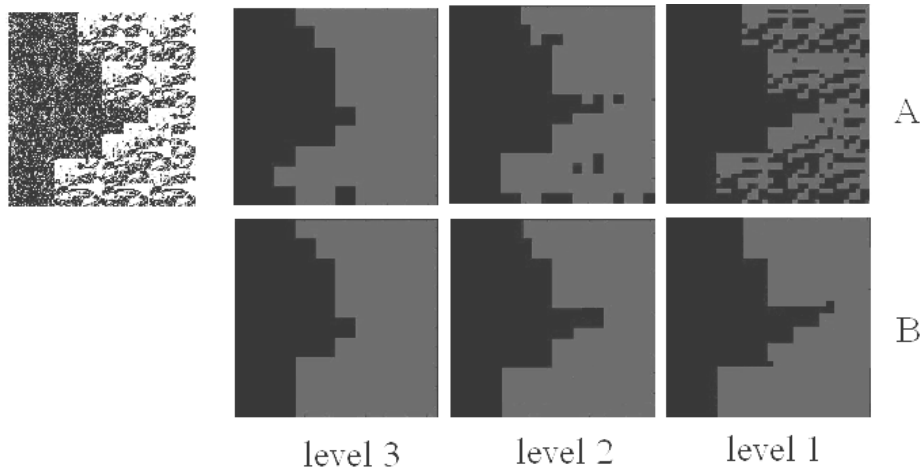


**Figure 3.** Multi resolution clustering with (A) and without (B) inter-scale decision using 10 by 10 window

The procedure of the clustering with inter-scale decision fusion is described below. Once clustering with  $V_{i+n}$  is completed, the mean and deviation at  $V_{i+n+1}$  of cluster based on the result at  $V_{i+n}$  are computed. These values of cluster centers are used as initial cluster center at  $V_{i+n+1}$  and normalized label value of  $V_{i+n}$  is added as one of input vector for clustering at  $V_{i+n+1}$ . In the same way, the values of cluster centers of  $V_{i+n+1}$  are used as initial cluster center at  $V_{i+n}$ . These steps are iterated until the clustering result of  $V_{i+n+1}$  is stable. After completing clustering at  $V_{i+n+1}$ , the same steps are repeated with  $V_{i+n+1}$  and  $V_{i+n+2}$ . Figure 3 shows the differences between the results in case of common clustering (A) and the ones in case of inter-scale decision fusion (B).

## TESTS AND DISCUSSIONS

To examine the suggested image segmentation algorithm, two rock images collected from MER PANCAM [Bell III et al, 2003] are used. The image consists of 1024 by 1024 pixels with 256 gray levels, with a focal length 43 millimeters and R1 filter (436nm). The images are taken by rover Spirit at the Gusev Crater landing site. The procedure of the test is depicted in the flow chart shown in Figure 4. In the preprocessing step, we decrease the effect of heterogeneous illumination through the low pass filter image subtraction. After that, shadows are removed based on two criteria that shadow has lowest intensity among the histogram clustering and does not include texture. Finally, we perform the image segmentation with schemes described above. Figure 5 shows the image segmentation result with multi-resolution histogram algorithm with a 16 by 16 window for texture estimator. The segmentation result is shown in Figure 5 (B) and result refined with inter-scale decision fusion is shown in Figure 5 (C). Another result of detected rocks is in Figure 6. The tests demonstrate satisfactory outcome for most of the regions in two MER rover images. Difficulty occurs at places where very small rocks are next to or between big rocks. The results can be utilized as initial locations for further refinement to delineate the exact rock boundary. This work can be applied to rover navigation to avoid obstacle, rock classification for scientific studies, and surface data training of satellite image on Mars.

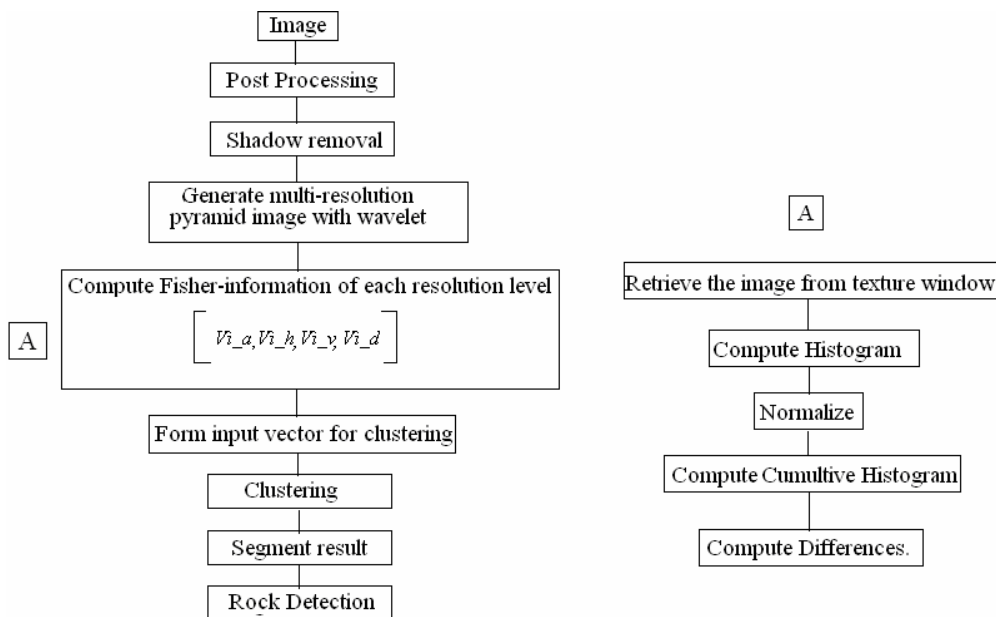


**Figure 4.** Workflow for rock segmentation with multi resolution clustering

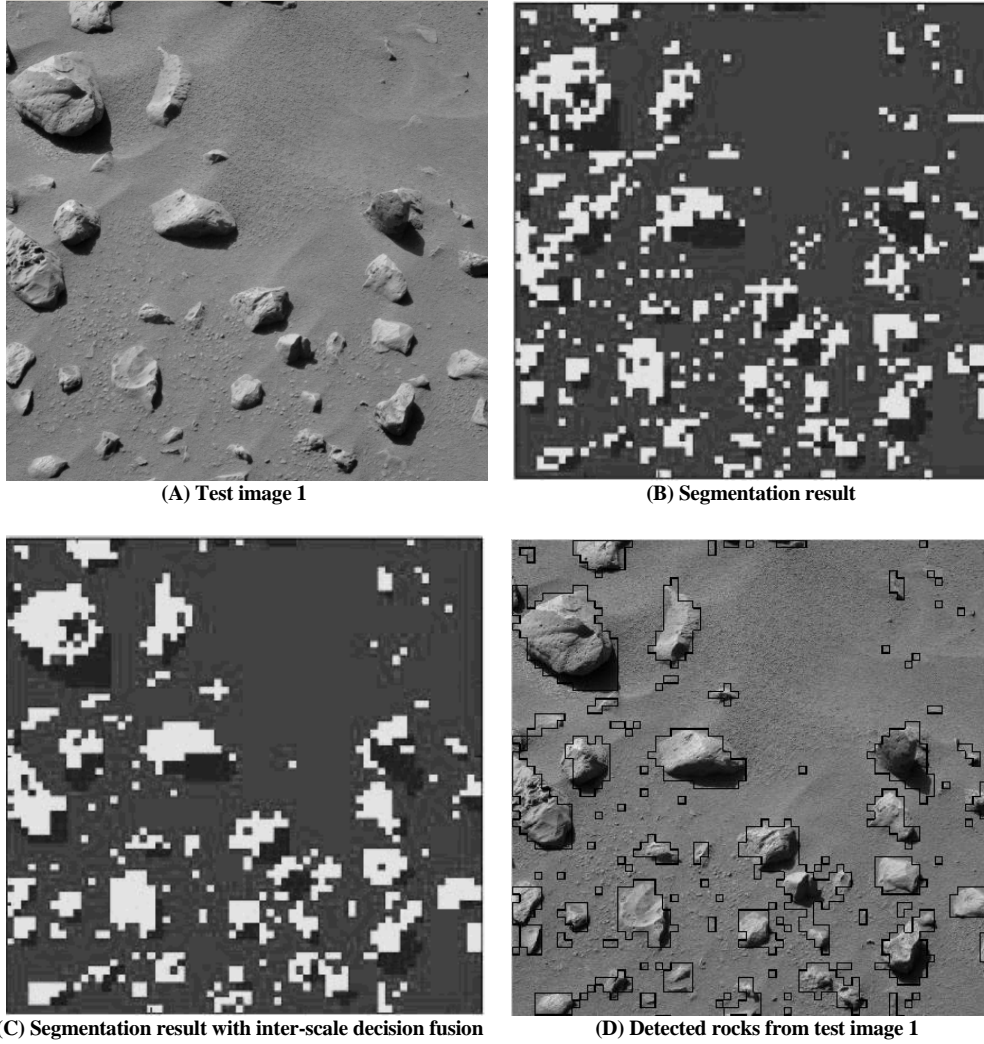


**Figure 5.** Image segmentation results and detected rocks (D) from test image 1

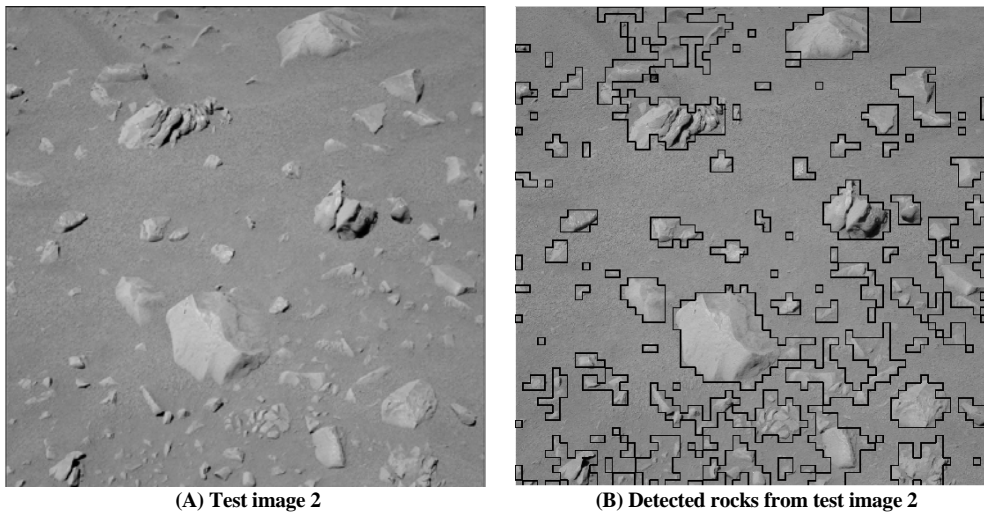


**Figure 6.** Detected rocks from test image 2

## REFERENCES

- J. F. Bell III, S. W. Squyres, K. E. Herkenhoff, J. N. Maki, H. M. Arneson, D. Brown, A. Collins, A. Dingizian, S. T. Elliot, E. C. Hagerott, A. G. Hayes, M. J. Johnson, J. R. Johnson, J. Joseph, K. Kinch, M. T. Lemmon, R. V. Morris, L. Scherr, M. Schwochert, M. K. Shepard, G. H. Smith, J. N. Sohl-Dickstein, R. J. Sullivan, W. T. Sullivan, and M. Wadsworth (2003), "Mars Exploration Rover Athena Panoramic Camera (Pancam) Investigation", *Journal of Geophysical Research*, vol. 108, no. e12 pp. 4.1-4.30
- A. Castano, R. Anderson, R. Castaño, T. Estlin, and M. Judd (2004), "Intensity-Based Rock Detection for Acquiring Onboard Rover Science", in *Proceedings of the 34th Lunar and Planetary Science Conference*
- F. S. Cohen, Z. Fan and M. A. Patel (1991), "Classification of rotation and scaled textured image using gaussian markov random field model", *IEEE Trans. Pattern Anal. Machine Intell. PAMI*, vol.13 no.2, pp 192-202
- R.C. Crida, R.C. & De Jager, G. (1994), "Rock recognition using feature classification." *Proceedings of the IEEE South African Symposium on Communications and Signal Processing*, pp. 152-157.
- C. Fosgate, H. Krim, W. Irving, W. Karl, and A. Willisky,(1997) "Multi-scale segmentation and anomaly enhancement of SAR imagery", *IEEE. Trans. Image Processing*, vo;6 pp 7-20
- V. Gor, R. Castano, R. Manduchi, R. C. Anderson, and E. Mjolsness (2001), "Autonomous Rock Detection for Mars Terrain", in *Proceedings of AIAA Space 2001*
- E. Hadjidemetriou, M. Grossberg, S. K. Nayar(2004) ,"Multiresolution Histograms and their Use for Recognition",*IEEE Transactions on Pattern Analysis and Machine Intelligence* vol.26 no.7, 831-847
- IEEE, 1990. IEEE Standard 610.4, <http://www.ing.unipi.it/~d9155/courses/vision/glossary.pdf>
- K. Jain, F. Farrokhanian (1991), "Unsupervised texture segmentation using Gabor filter", *Pattern recognition*, vol.24 no.12 pp. 1167-1186
- R.L. Kashyap and A. Khotanzad,(1986) " a model-based method for rotation invariant texture classification", *IEEE Trans. Pattern Anal. Machine Intell. PAMI*, vol.8 no.4, pp 471-481]
- J. Li, R.M. Gray, and R.A.Olshen,(2000)"Multi-scale image classification by hierarchical modeling with two dimensional hidden Markov models", *IEEE Trans. Inform. Theory*, vol.46 no.5 pp1826-1841
- E. Salari and Z. Ling (1995), "Texture segmentation using hierarchical wavelet decomposition," *Pattern Recognition.*, vol. 28, pp. 1819–1824, Dec. 1995.
- D. Thompson, S. Niekum, T. Smith, and D. Wettergreen (2005)"Automatic Detection and Classification of Features of Geologic Interest", in *Proceedings of IEEE Aerospace Conference*, 2005.
- M. Vlachos, J. Lin, E. Keogh, D. Gunopulos (2003). ,"Multi-Resolution K-Means Clustering of Time Series and Application to Images". In *proceeding of the 4th SIGKDD Workshop on Multimedia Data Mining*